7th International Conference on Structures in Fire
M. Fontana, A. Frangi, M. Knobloch (Eds.)
Zurich, Switzerland, June 6-8, 2012

HIGH TEMPERATURE TESTS ON PARTIALLY ENCASED BEAMS

Paulo A. G. Piloto*, Ana B. R. Gavilán, Luís M. R. Mesquita* and Carlos Gonçalves***

* IDMEC, Polytechnic Institute of Bragança, Portugal
e-mails: ppiloto@ipb.pt, lmesquita@ipb.pt, carlosajgoncalves@gmail.com

** University of Salamanca, Spain
e-mail: aramos@usal.es

Keywords: Partially encased beams, High temperature, Experimental tests, Bending resistance.

Abstract. *Partially encased beams (PEB) are composite steel and concrete elements that present several advantages with respect to steel bare elements. This paper presents a set of experimental tests developed using two different beam lengths and two different shear conditions between stirrups and web (W – welded and NW – not welded), at high temperature (200, 400, 600 ºC) and room temperature. The composite section was built-up with IPE100 steel profile and reinforced concrete between flanges. The deformed shape mode and the bending resistance were compared for different temperature levels and stirrup shear conditions (W and NW). The behaviour of PEB was also compared with bare steel at room temperature. Most of the beams attained the ultimate limit state by lateral torsional buckling (LTB), with exception for those tested at 600 ºC, which collapsed by the formation of a plastic hinge (PH).*

1 INTRODUCTION

PEB have been widely tested at room temperature, but only a small number of testes are reported under fire or under high temperature. The most relevant tests were developed by Kindmann et al [1], proving the importance of the reinforced concrete between flanges for bending resistance. Lindner and Budassis in 2000 [2] developed a new design proposal for lateral torsional buckling. Maquoi et al [3], improved the knowledge on the elastic critical moment and on the lateral torsional buckling resistant moment. Makamura et al. [4], tested 3 partially encased girders with longitudinal and transversal rebars (W and NW) to flanges, concluding that bending strength of the PEB was almost two times higher than conventional bare steel girders and specimens with rebar not welded to flanges presented a decrease of 15 % for maximum load bearing when compared to the welded rebar (W) specimens.

PEC (partially encased columns) were also tested at room and elevated temperatures. Hunaiti et al. [5], analysed the behaviour of 19 PEC without additional shear connectors, and tested those fabricated with shear connectors and batten plates for different loading conditions. All columns presented full composite action and similar strength, regardless of the type of additional steel. Stefan Winter and Jörg Lange [6], determined the ultimate load of 8 PEC at room temperature using high strength-steel. Authors developed some full scale tests under fire conditions and concluded for equal ultimate load for both materials. Brent and Robert [7], investigated the behaviour of PEC, comparing the performance of High Strength Concrete (HSC) and Normal Strength Concrete (NSC), evaluating the ultimate load and failure mode. Authors verified that PEC with HSC had more brittle failure mode than NSC, concluding that introducing steel fibres and reducing spaces between stirrups would improve ductility. A. Correia and João P. Rodrigues [8], studied the effect of load level and thermal elongation restraint on 3.0 m length PEC, built with HEA 160 and HEA 200, under fire conditions. They concluded that the surrounding stiffness had a major influence on fire element behaviour for lower load levels. The increasing of the surrounding stiffness is responsible for reducing critical time. Critical time remains practically unchanged for higher load levels.

A small number of 15 experiments were already developed on PEB under fire conditions (small series) to determine fire resistance, reported by authors in a previous work [9]. This current work intends to present high temperature tests for medium and large series, using the same cross section type with two different lengths, three different temperature levels of 200, 400 and 600 ºC, calculating bending resistance.

2 SPECIMENS

PEB were prepared by filling the space between the flanges of a steel IPE100 profile, using reinforced concrete (RC). Partially encased sections achieve higher fire resistance when compared to bare steel sections. The increase in fire resistance is due to the encased material, reducing the exposed steel surface area, introducing concrete which has a low thermal conductivity. Higher fire resistance can also be achieved by increasing the amount of reinforcement to compensate for the reduction of steel strength in case of fire, as reported by several researchers.

Two different shear configurations for stirrups were used, both represented in figure 1. According to EN1994-1-1 [10], this composite steel and concrete section is classified as class 1.

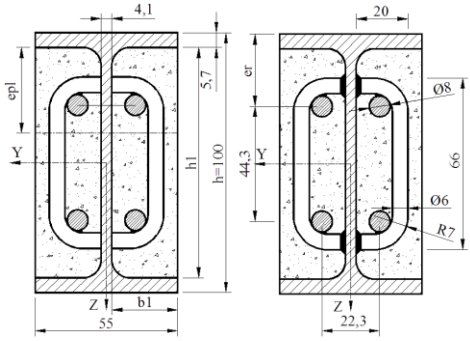

Figure 1. Cross section geometry

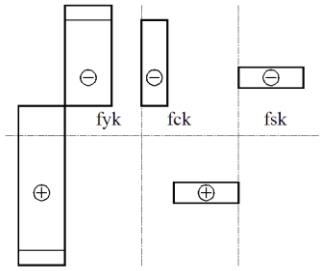

Figure 2. Plastic stress distribution in cross section

The plastic neutral axis is referenced to “epl”, reinforced concrete block dimensions are represented by “b1” and “h1”, while “er” represents the relative position for reinforcement.

According to EN1994-1-2 [11], member analysis under fire conditions may be verified using either tabulated data, simplified or advanced calculation methods. Tabulated data refers only to composite beams rather than PEB, depends on load level, and is only valid for standard fire exposure and simple supporting conditions. A simple calculation method may be used to determine fire resistance of PEB without shear connection to the concrete slab. The rules for composite beams may be applied to PEB, assuming no mechanical resistance of the reinforced concrete slab, and establishing reduced effective areas of the cross section. An advanced calculation method may also be used to analyse partially encased beams. These models may include separate calculation programs for temperature and displacement.

In order to define load level dependence for partially encased sections at room temperature, the plastic moment was calculated using characteristic values for material properties, assuming certain hypotheses based on stress field distribution, see figure 2 and eq. 1, [2].

The plastic moment at room temperature was calculated, assuming that the effective area of the steel profile may be stressed in compression and tension, up to its characteristic yield strength (f_{yk}); the effective area of longitudinal reinforcement (A_s) may be stressed to their characteristic yield strength (f_{sk}) in tension and compression, and the effective area of concrete in compression may be stressed up to the characteristic value of concrete cylinder compressive strength f_{ck}, constant over the compressive part of concrete. The contribution of IPE100 bare steel to the plastic moment is equal to 80%, while the contribution of RC to the plastic moment represents 20%.

$$M_{pl} = W_{pl,y}.f_{yk} - 2.f_{yk}.t_w.\left(0.5h_1 - e_{pl}\right)^2 \Big/ 2 + f_{ck}.2.b_1.e_{pl}\left(0.5h_1 - 0.5e_{pl}\right) + 2.A_r.\left(f_{sk} - f_{ck}\right)\left(h - 2.e_r\right) \quad (1)$$

The shear resistance was also verified at room temperature. The contribution of web encasement to shear may be taken into account if stirrups are fully welded to the web, otherwise shear reinforcement should not be considered. The distribution of the total shear resistance into steel resistance and RC resistance may be assumed to be in the same proportion as it is for bending resistance, [10]. The design resistance for bending and shear were determined by 14.8 kNm and 102 kN. These limits helped to decide about the capacity of the hydraulic jack to be used.

PEB were made of IPE100 with steel S275 JR, using C20 encased concrete with siliceous aggregates. Four longitudinal steel B500 rebar were used with diameter of 8 mm. Stirrups were designed with B500 rebar with a diameter of 6 mm, spaced every 167 mm. Stirrups were also partially welded to the longitudinal steel reinforcement, as represented in figure 1.

3 EXPERIMENTS

Twenty PEB and two bare steel beams were tested under four-point bending. Tests were grouped in eight series to determine bending resistance at different temperature levels. Two series were prepared to analyse the behaviour of stirrups not welded to the web (NW), four series were prepared for high temperature levels using welded stirrups (W) and two series were defined to be tested at room temperature. Two slenderness ratio were considered, using beams with Lt=2.5 m and Lt=4.0 m. Three tests were defined for high temperature series, with exception for series 7 and 8, see table 1.

Table 1. List of partially encased beams to be tested (specimens).

Series	Specimen	Length Ls [m]	Stirrups [W/NW]	Temp. [ºC]	Max. impe. [mm]
1	B/2.4-01	2.4	W	400	2
	B/2.4-02				2
	B/2.4-03				2
2	B/2.4-04	2.4	W	200	1
	B/2.4-05				2
	B/2.4-06				1
3	B/2.4-07	2.4	NW	400	1
	B/2.4-08				1
	B/2.4-09				1
4	B/3.9-01	3.9	W	400	2
	B/3.9-02				5
	B/3.9-03				3
5	B/3.9-04	3.9	W	600	2
	B/3.9-05				2
	B/3.9-06				5
6	B/3.9-07	3.9	NW	400	5
	B/3.9-08				5
	B/3.9-09				2
7	B/3.9-11	3.9	W	room	2
	B/3.9-12				5
8	B/3.9-11A	3.9	W	room	1
	B/3.9-12A				3

Table 1 identifies each PEB tested, the length between supports (L_s), the shear condition for stirrups, the maximum temperature used during heating and the maximum geometric imperfection. The initial out-of-straightness was measured using a laser beam.

Specimens were tested using a steel portal frame, see figure 3. Room temperature tests were developed in one single stage, using small increments of load, while high temperature tests were developed in two stages. The first stage was used for heating the beam along the length "Lf", using a constant heating rate and a dwell time for constant temperature. During the second stage, temperature was kept constant and load was slowly increased.

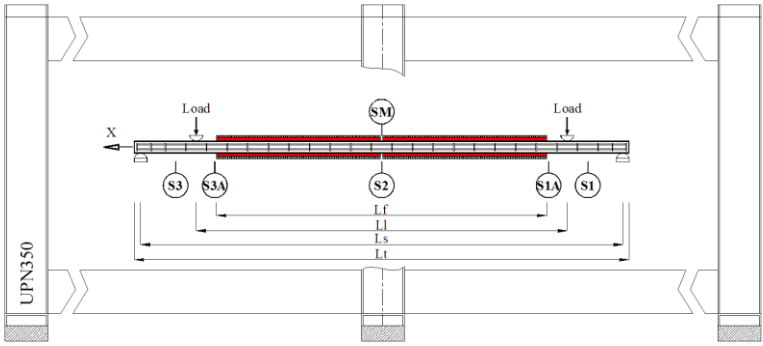

Figure 3. Testing conditions and main cross sections.

Five different cross sections were defined to measure temperature (S1, S1A, S2, S3A and S3), in case of high temperature tests and one cross section was used to measure strain (SM at room temperature), displacements (vertical Z_G, lateral Y_G) and cross section rotation θ_G.

Table 2 defines the lengths for medium and large test series.

Table 2. Lengths defined for each beam (specimen).

Specimen	Total length Lt [m]	Length supports Ls [m]	Length load Ll [m]	Heating length Lf [m]
B/2.4	2.5	2.4	1.5	1.3
B/3.9	4.0	3.9	3.0	2.8

Two fork supports were applied on each four-point bending test. Restraint against Y/Z displacement and restraint against X rotation was considered at each support. A special interface was developed to apply vertical load, introducing a certain level of restrain against X rotation but allowing for lateral displacement Y. Teflon was used to reduce friction between the beam and the hydraulic jack. see figure 4.

Figure 4. Testing supports with load cell (left) and load applied by the hydraulic jacks (right).

The distance between load and support was kept constant for large and medium series. The length of specimens to be heated was shorter than the length between supports. This effect may be negligible

because bending moment is reduced in the region nearest the supports and will not be affected by heating. Free thermal elongation was allowed before adjusting both supports and starting with each test.

3.1 Materials

Each material was characterized according to international standards [12] for hot rolled and cold formed steel, see table 3. Three samples were collected from the web of steel hot rolled profile and two more samples were collected from steel reinforcement.

Table 3. Tensile tests for hot rolled and cold formed steel.

Properties	Steel profile		Steel reinforcement	
	Average	Std. Deviation	Average	Std. Deviation
E [GPa]	197.901	2.948	203.294	2.110
$R_{p.0.2\%}$ [MPa]	300.738	6.720	524.993	3.521
ReH [MPa] (f_{yk}) (f_{sk})	302.466	5.749	531.508	7.908
ReL [MPa]	300.856	4.028	520.825	4.068
Rm [MPa] (fu)	431.252	5.020	626.574	11.539
At [%]	41.584	0.231	25.155	0.495

E- Elastic modulus, $R_{p.0.2\%}$- proof strength for 0.2%, ReH- upper yield strength, ReL- lower yield strength, Rm- tensile strength, At- total extension at the moment of fracture.

Concrete was made with Portland cement, sand and siliceous aggregates. The concrete composition was prepared according to table 4. Aggregates (gravel and sand) were characterized by the sieving method and tested according to international standard [13] to determine particle size dimension. Due to the small size of the steel section and considering the offset dimension for the concrete cover of the stirrups, the concrete was made up with small-sized aggregates. The percentage of aggregates with diameters between 4-6 mm was 90%, while the percentage of sand with diameters between 0.063-0.5 mm was 80%. The aggregate dimensions limit the value of the compressive resistance of concrete as concluded by Keru et al, [14]. The high level of permeability at elevated temperature was responsible for decreasing pore pressure. This fact justifies the absence of explosive spalling.

Table 4. Mix proportions of concrete.

Component for	1 [m^3] concrete
Sand	1322.7 [kg]
Aggregates	451.1 [kg]
Water	198 [l]
Cement	466.7 [kg]
Water / Cement	45 %

Table 5 shows the results for the compressive strength of concrete, using three compressive tests for cubic samples ($f_{ck,cube}$) and three compressive tests for cylindrical samples (f_{ck}).

Table 5. Compressive tests results for concrete.

Properties	Cure [days]	Average	Std. Deviation
$f_{ck,cube}$ [MPa]	29	21.45	1.03
f_{ck} [MPa]	29	20.36	0.30

An increase of 100% on the compressive strength of concrete would lead to an increase of 2% in the bending resistance of PEB at room temperature. This means that this section type is not sensitive to the value of the compressive strength of concrete.

3.2 Instrumentation

PEB were prepared to be tested at room temperature, measuring strain in central section (SM). Figure 5 represents the location for strain gauges, over steel flange and web, in hot rolled section (SM-WS and SM-OS) and over concrete (SM-RC1 and SM-RC2). Whereas perfect bond was considered between concrete and reinforcement, concrete strain was measured on steel reinforcement; for the latter measurement, rebars were machined 1 mm in depth and 15 mm in length, in respect to the dimensions of the electrical strain gauge. Five strain gauges (HBM reference 1-LY11-3/120) were used. All strain gauges were protected with gloss and special viscous putty (HBM reference Ak22) against moisture, water and mechanical damage.

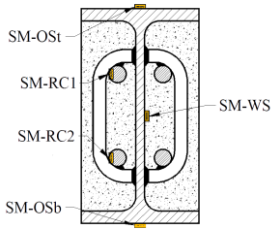

Figure 5. Strain gauge positions for steel and concrete.

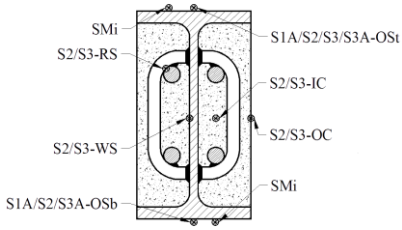

Figure 6. Thermocouple positions for all cross sections

PEB were also prepared to be tested at high temperatures, using thermocouples type K positioned along the length of each element, according to figure 6. Thermocouples were positioned in place, using the spot welding machine. For the concrete temperature measurements, positions Si-IC and Si-OC, thermocouples were welded to a small steel washer, wrapped in concrete.

3.3 Testing procedures

Tests developed at room temperature used quasi-static load increments, based on load cell readings. Load was applied with two synchronized hydraulic jacks. Strain, displacement and cross section rotation were determined at central section (SM). Transversal and lateral displacements (Z_G, Y_G) as well as cross section rotation were based on three wire potentiometric displacement transducers. Some important force events were recorded for each test. The force value for plastic moment (F_{Mpl}) was determined using the intersection method between two straight lines drawn from linear and non-linear interaction. The load event for transversal displacement equal to L/30 was also determined ($F_{L/30}$) and the maximum load level for the asymptotic behaviour of the transversal displacement was identified by (Fu).

Tests developed at elevated temperature used electro-ceramic heating device to increase and sustain temperature during loading. A heating rate of 800 ºC/hour was applied, which lead to heating periods of 15, 30 and 45 minutes. An insulation ceramic mat was applied to increase heating efficiency. Supports were adjusted and load was applied after temperature stabilization (60, 90 and 120 minutes after the start of heating). The same procedure was used to measure transversal and lateral displacement, as well as, cross section rotation. Load events were also recorded as well and temperature measurements in the main cross section.

4 RESULTS

Four-point bending tests were performed to evaluate bending resistance of PEB at high and room temperature. Bending resistance was also compared to bare steel beams, using the same cross section for steel. Two different beam lengths were tested (medium and large series). Two different conditions were tested for stirrups (W and NW) at elevated temperature (400 ºC). Several performance criteria were defined to compare the effect of different conditions. Force events were defined when the cross section became plastic (F_{Mpl}), when the transversal displacement reached L/30 ($F_{L/30}$) and when force reached its

maximum value (F_u). Temperature evolution in time was represented for certain periods of time and temperature distribution over each beam length was also represented.

4.1 Bending resistance of PEB (medium series)

The medium series includes results of PEB with Ls=2.4 m. All tested beams reached lateral torsional buckling as deformed shape mode. Figures 7-12 present the results for PEB with welded stirrups.

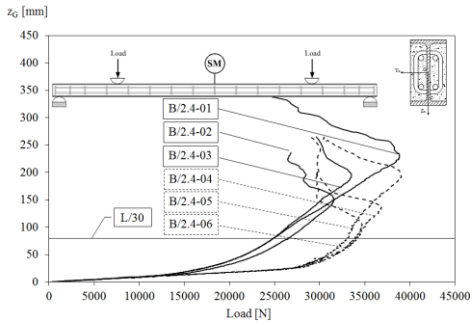

Figure 7. Deflection behaviour at mid span for series 1/2.

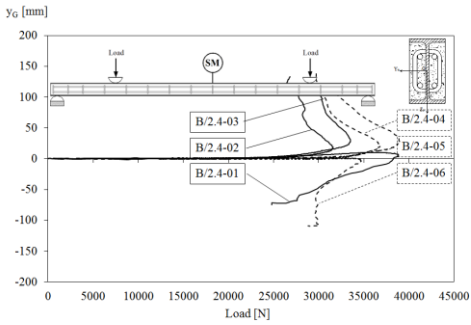

Figure 8. Lateral displacement for series 1/2.

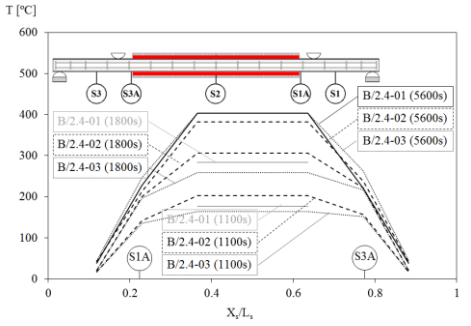

Figure 9. Temp. distribution and evolution for series 1.

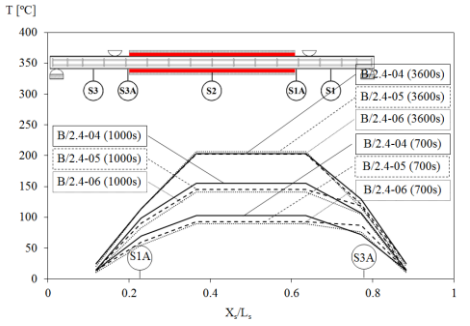

Figure 10. Temp. distribution and evolution for series 2.

Figure 11. Deformed shape mode for B/2.4-01.

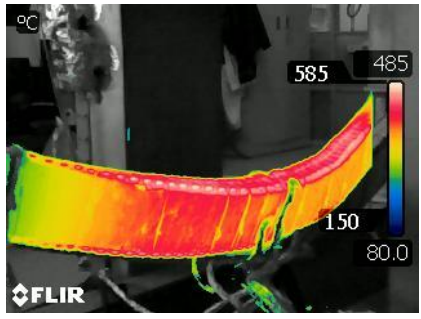

Figure 12. Temperature at the end of test for B/2.4-01.

Displacement results were determined for PEB with stirrups NW. Series 3 presented almost the same behaviour as series 1. Table 6 presents the main force events during each test for medium series. The results agree very well with exception for the ultimate load (Fu). Differences may be explained by the friction effect near the supports / load and by the deformation mode shape developed at high load level.

Table 6. Force results for medium series.

Series	Specimen	F(Mpl) [N]	F(L/30) [N]	Fu [N]
1	B/2.4-01	18890	24932	38864
	B/2.4-02	21760	26583	31533
	B/2.4-03	19920	24878	33568
2	B/2.4-04	31430	34060	36875
	B/2.4-05	30350	32953	39042
	B/2.4-06	31380	33930	34712
3	B/2.4-07	20610	24898	29000
	B/2.4-08	19270	25135	40861
	B/2.4-09	20850	25722	33246

4.2 Bending resistance of PEB (large series)

The large series includes results of PEB with Ls=3.9 m. Figures 13-18 present the results for transversal and lateral displacements. Results agree very well with each other, with exception to the end of the tests. Temperature evolution and distribution is also plotted in graphs. Temperature is not uniform along the beam because the insulation is not perfect and heat flows by conduction, mainly along the steel part of PEB. The deformed shape mode for series 4 was lateral torsional buckling. Plastic hinge formation was the dominant deformed shape mode verified for series 5. Some lateral displacement did also occur.

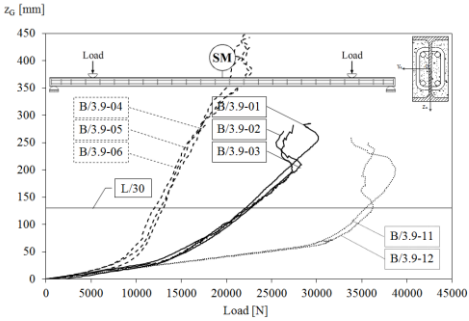

Figure 13. Deflection behaviour at SM for series 4/5/7.

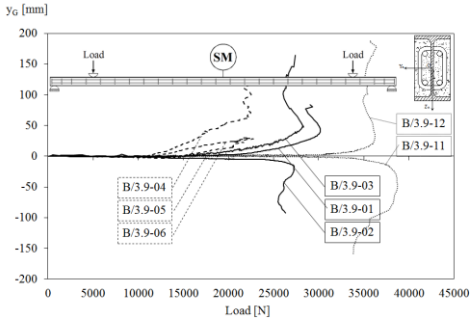

Figure 14. Lateral displacement at SM for series 4/5/7.

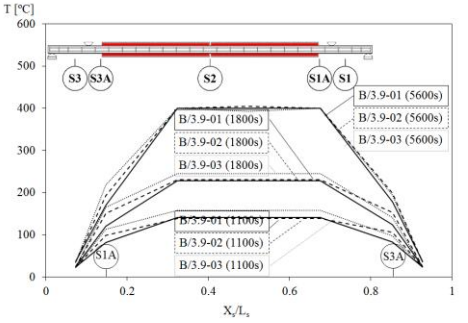

Figure 15. Temp. distribution and evolution for series 4.

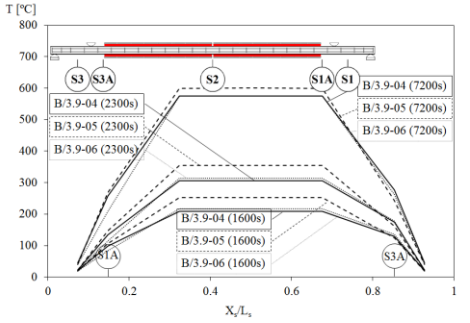

Figure 16. Temp. distribution and evolution for series 5.

Figure 17. Deformed shape mode for B/3.9-05.

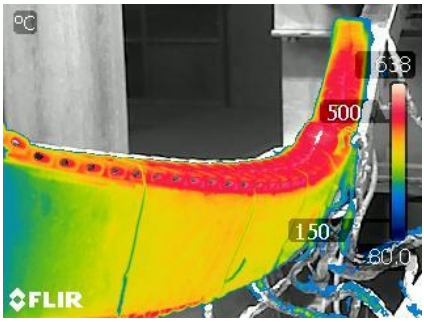

Figure 18. Temperature at the end of test for B/3.9-07.

Displacement results were determined for PEB with stirrups NW. Series 6 presented results in agreement with series 4. Table 7 presents the main force events during each test. The results agree very well with exception for the ultimate load (Fu). Differences may be explained as discussed previously.

Table 7. Force results for large series.

Series	Specimen	F(Mpl) [N]	F(L/30) [N]	Fu [N]
4	B/3.9-01	16370	22126	30204
	B/3.9-02	16360	22715	27290
	B/3.9-03	14850	22573	28337
5	B/3.9-04	9620	12641	22456
	B/3.9-05	9759	12996	21662
	B/3.9-06	9110	12025	22770
6	B/3.9-07	15000	22665	23591
	B/3.9-08	15600	24234	32642
	B/3.9-09	15100	23207	24816
7	B/3.9-11	31600	35428	38718
	B/3.9-12	32100	36161	36380
8	B/3.9-11A	-	-	19436
	B/3.9-12A	-	-	21272

5 CONCLUSIONS

Four-point bending tests were performed to evaluate bending resistance of PEB at high and room temperature. Force and displacement results are presented to compare bending resistance. The bending strength of the PEB at room temperature is almost two times the bending resistance of bare steel beam. The reduction on bending resistance of PEB is not directly proportional to the increase of temperature. An increase of temperature form 200ºC to 400 ºC leads to a reduction of 24 % on F(L/30) for medium series, while an increase from room to 400ºC, 600ºC leads to a reduction of 37 % and 64% on F(L/30), respectively.

The deformed shape mode was LTB for all tested PEB and bare steel beams, with exception to those tested at 600 ºC.

ACKNOWLEDGMENT

Authors acknowledge material support to the following companies: Arcelor – Mittal (Spain), J. Soares Correia (Portugal), Fepronor (Portugal) and Hierros Furquet (Spain).

REFERENCES

[1] R. Kindmann, R. Bergmann, L-G. Cajot, J. B. Scleich; "Effect of reinforced concrete between the flanges of the steel profile of partially encased composite beam"; *Journal of Constructional Steel Research*, 27, pp 107-122, 1993.

[2] Joachim Lindner, Nikos Budassis; "Lateral torsional buckling of partially encased composite beams without concrete slab"; *Composite construction in steel and concrete IV, conference proceedings*, May 28th to June 2nd , Banff, Alberta, Canada, 2000.

[3] R. Maquoi, C. Heck, V. Ville de Goyet, et al, (European commission), "Lateral torsional buckling in steel and composite beams"; ISBN 92-894-6414-3; Book 1,2 and 3; *Technical steel research final report EUR 20888 EN*; August 2002.

[4] S. Nakamura, N. Narita, "Bending and shear strengths of partially encased composite I-girders", *Journal of Constructional Steel Research*, 59, pp.1435-1453, 2003.

[5] Hunaiti, Y.; Fattah, B. A.; "Design considerations of partially encased composite columns", *Proceedings Institution of Civil Engineers Structures & Buildings*, v.106, pp.75-82, Feb. 1994.

[6] Stefan Winter and Jörg Lange, "Behavior of Partially Encased Composite Columns Using High-Strength Steel – Service and Fire Condition", *Proceedings of the Conference, "Composite Construction IV"*, Banff, Canada, 2000.

[7] Brent Pricket, Robert Driver, "Behaviour of partially encased composite columns made with high performance concrete", *Structural Engineering report nº 262*, University of Alberta, Department of Civil & Environmental Engineering, 2006.

[8] António J.P. Moura Correia, João Paulo C. Rodrigues, "Fire resistance of partially encased steel columns with restrained thermal elongation", *Journal of Constructional Steel Research*, Volume 67, Issue 4, pp. 93-601, April 2011.

[9] Paulo A. G. Piloto, Ana B. R. Gavilán, Luís M. R. Mesquita; "Temperature analysis on fire resistance experiments of partially encased beams"; *Safety and Security Engineering IV*, pp. 313-324, WIT Press, ISBN 978-1-84564-522-9, ISSN: 1746-4498 (print), ISSN:1743-3509 (on-line), University of Antwerp, Belgium, 4-6 July 2011.

[10] CEN - EN 1994-1-1; *"Eurocode 4: Design of composite steel and concrete structures - Part 1-1: General rules and rules for buildings"*; Brussels, December 2004.

[11] CEN - EN 1994-1-2; *"Eurocode 4: Design of composite steel and concrete structures - Part 1-2: General rules - Structural fire design"*; Brussels, August 2005.

[12] ISO TC 164, ISO 6892-1; "*Metallic materials – tensile testing – part 1: Method of test at room temperature"*; Switzerland, international standard, 2009.

[13] IPQ (Instituto Português da Qualidade), NP EN 933-1, *"Tests for geometrical properties of aggregates – part 1; Determination of particle size distribution, sieving method"*, 2000.

[14] Keru Wu, Bing Chen, Wu Yao, Study of the influence of aggregate size distribution on mechanical properties of concrete by acoustic emission technique, *Cement and Concrete Research*, Volume 31, Issue 6, pp. 919-923, May 2001.